Article

Dependence of GaN Exciton Energy on Temperature

Xiancheng Liu, Peng Chen *, Zili Xie, Xiangqian Xiu, Dunjun Chen, Hong Zhao, Yi Shi, Rong Zhang and Youdou Zheng

Key Laboratory of Advanced Photonic and Electronic Materials, School of Electronic Science and Engineering, Nanjing University, Nanjing 210093, China; liuxiancheng05@163.com (X.L.); xzl@nju.edu.cn (Z.X.); xqxiu@nju.edu.cn (X.X.); djchen@nju.edu.cn (D.C.); zhaohong@nju.edu.cn (H.Z.); yshi@nju.edu.cn (Y.S.); rzhang@nju.edu.cn (R.Z.); ydzheng@nju.edu.cn (Y.Z.)
* Correspondence: pchen@nju.edu.cn

Abstract: In this paper, we investigate the relationship between GaN exciton energy and temperature by using high-quality, strain-free GaN epilayers. Traditional models, such as Varshni's model and the Bose–Einstein model, are primarily based on empirical fitting and give little or no consideration to electron–phonon interactions, which prevents them from accurately calculating GaN exciton energy over a wide temperature range. Considering the interaction of electrons and phonons, we use singular functions, linear functions and power functions to express the phonon density of GaN, and then 2BE, singular-linear, power-law-delta, and power-law-v models are proposed. All of them provide results that are more consistent with actual measurements compared to traditional models. Among them, the singular-linear model summarizes the contributions of acoustic and optical phonons. The error associated with the singular-linear model is smaller than that of the 1BE and Varshni models across nearly the entire temperature range. Therefore, the singular-linear model is a better choice.

Keywords: GaN; exciton energy; temperature; modes

Academic Editor: Dmitri Donetski

Received: 6 January 2025
Revised: 16 January 2025
Accepted: 24 January 2025
Published: 26 January 2025

Citation: Liu, X.; Chen, P.; Xie, Z.; Xiu, X.; Chen, D.; Zhao, H.; Shi, Y.; Zhang, R.; Zheng, Y. Dependence of GaN Exciton Energy on Temperature. *Crystals* **2025**, *15*, 137. https://doi.org/10.3390/cryst15020137

Copyright: © 2025 by the authors. Licensee MDPI, Basel, Switzerland. This article is an open access article distributed under the terms and conditions of the Creative Commons Attribution (CC BY) license (https://creativecommons.org/licenses/by/4.0/).

1. Introduction

In recent decades, many groups have studied the relationship between the energy bands of semiconductor materials and temperature [1–7]. These studies provide valuable insights into the dependence of the energy band on temperature, which is a crucial prerequisite for accurately understanding the optical and electrical properties of semiconductor materials. For these traditional materials, such as Si, Ge, GaAs, InP, etc., many groups have systematically studied the dependence of their exciton energy on temperature and have achieved great results [8–14]. However, over the years, in the field of wide bandgap semiconductor materials, particularly GaN, has faced challenges in obtaining high-quality GaN samples due to the lack of effective preparation methods. As a result, the systematic study of GaN materials has been limited by the presence of high defects, resulting in unclear findings regarding some of its intrinsic properties, including the relationship between the GaN bandgap and temperature. In recent years, fortunately, the rapid development of MBE and MOCVD growth technologies and the fabrication of GaN freestanding substrate have enabled us to produce high-quality GaN, which provides the material basis for our research on GaN [15].

Group III nitrides represented by GaN have a wide range of applications in optoelectronics and power electronics [16–20]. Owing to its superior material properties such as high electric breakdown field, high chemical stability, and high mobility, GaN has been

extensively utilized in high-frequency and high-power devices, particularly those operating under elevated temperatures [21,22]. Therefore, establishing an accurate correlation between the bandgap width of GaN and temperature is crucial for device design. In this process, the electron–phonon interactions in GaN become the primary factor affecting the bandgap width. This study is based on measurement results from high-quality GaN, comparing various phonon models to derive the best relationship.

In typical measurements, the bandgap is determined by measuring the energy of band edge excitons. Several studies have already been conducted on the relationship between the exciton energy and temperature. To describe the behavior of exciton energy with temperature, it is widely accepted that exciton energy exhibits a quadratic dependence at low temperatures and a linear relationship at high temperatures [23,24]. In recent years, some groups have found that excitonic energy exhibits new behavior at low temperatures [25–27]. At a low temperature of 4 K, it has been found that the exciton energy of silicon is mathematically related to the temperature raised to the 4th power. For the factors that affect the exciton energy of semiconductor materials at ultra-low temperatures, many groups have conducted detailed investigations and achieved some results [28].

Some groups have also studied the dependence of GaN exciton energy on temperature with the traditional models, such as the Varshni and the Bose–Einstein models [29–33]. However, the fitting results are not satisfactory because traditional empirical models, which typically consist of only three empirical parameters, fail to account for the underlying physical mechanisms. This limitation can lead to inaccuracies in the predicted behavior of exciton energy as a function of temperature. As a result, there is a need for more comprehensive models that incorporate relevant physical principles, especially electron–phonon interactions, to better describe the relationship between exciton energy and temperature, particularly in a wider temperature range. Although the phonon models and density of states in GaN have not been fully studied, we can conduct various calculations based on existing research results to obtain a model that best fits the measurement results. In this paper, we consider electron–phonon interactions and, based on various phonon calculation models, employ singular functions, linear functions, and power functions to express the phonon density of GaN. Specifically, we propose the 2BE model, single-linear model, power-law delta model, and power-law-v model. The error of almost all electron–phonon interaction models is smaller than that of the Varshni model over nearly the entire temperature range. This suggests that the newly proposed electron–phonon interaction models can more accurately study the dependence of GaN exciton energy on temperature compared to traditional models.

2. Experiments

To obtain an accurate value for the band edge luminescence energy, it is essential to eliminate material defects, internal strain, and other factors that may affect the energy of the band edge. Therefore, high-quality GaN epitaxial materials are indispensable. In this work, we use 400 μm thick freestanding GaN substrates to realize high-quality and strain-free GaN epilayers using metal–organic chemical vapor deposition (MOCVD). Trimethylgallium and NH_3 were used as Ga and N sources, respectively. H_2 was the carrier gas. The reactor pressure was maintained at 200 Torr. Before growing the GaN epilayer, high temperature annealing was performed to clean the GaN substrate surface in NH_3 and H_2 mixed ambient at 1050 °C. Since there is no mismatch between the substrate and the epilayer, we can directly grow the GaN epilayer at 1020 °C after the surface cleaning up to 4 μm thick. However, for the GaN layer grown on sapphire substrate, it requires a buffer layer to overcome the mismatch between the GaN and sapphire. A 20 nm GaN buffer layer must first be grown at 520 °C on the sapphire substrate. Then, the buffer layer

is recrystallized when the temperature ramps to 1050 °C. After the recrystallization, the normal GaN epilayer can be grown up to 4 µm thick. Although we keep the major growth conditions same as those for the GaN substrate, high-density dislocations can be generated by the growth mode on the sapphire substrate, resulting in broader XRD peaks.

As shown in Figure 1a,b, the high-resolution XRD measurement results show that the crystal quality of the GaN epilayer grown on the freestanding GaN substrate (GaN/GaN) show a great improvement. It is well known that normal GaN grown on a sapphire substrate shows dislocation densities as high as $10^9/cm^2$ [34]. As a comparison, for a normal GaN layer grown on a sapphire substrate (GaN/sapphire), the full width at half maximum (FWHM) of the (0002) diffraction peak is more than 400 arc seconds, and it is more than 600 arc seconds for the (10–11) diffraction peak. However, for the GaN layer grown on the GaN substrate, the FWHM is only 62 arcseconds and 42 arcseconds for the corresponding diffraction peaks. The GaN/GaN sample shows extremely low dislocation density—as low as $10^5/cm^2$—as calculated from the high-resolution XRD results. Furthermore, the Raman scattering measurement (not shown here) proves that the GaN layer grown on the GaN substrate is totally strain free. The Hall measurement shows very low unintentional doping concentration as low as $10^{15}/cm^3$ in the high-quality GaN epilayer.

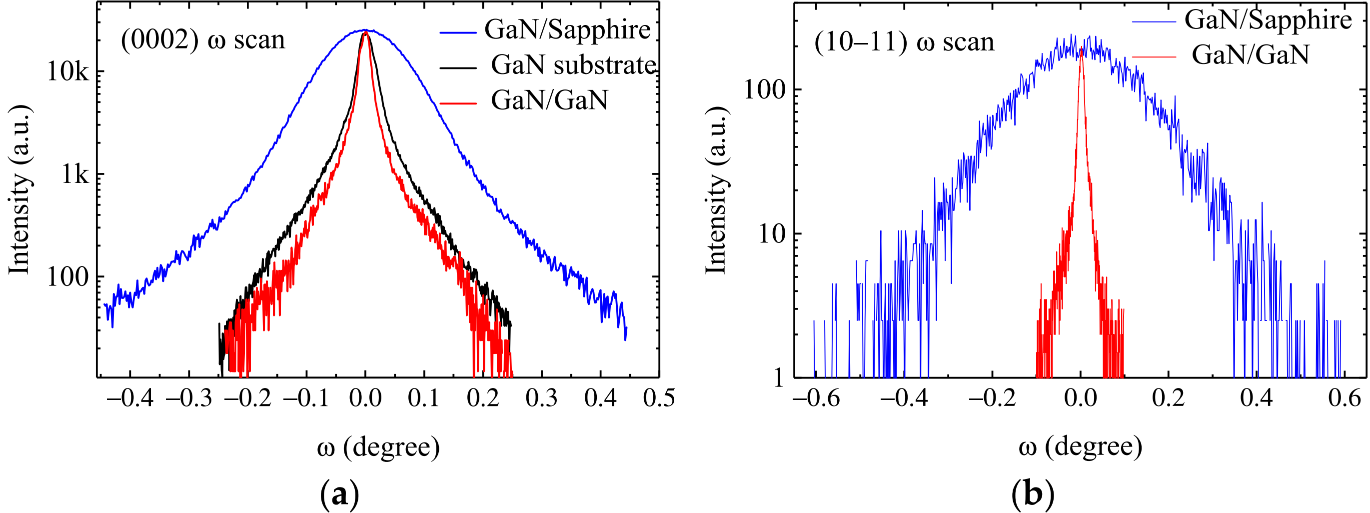

Figure 1. Comparison of crystal quality between GaN/sapphire and GaN/GaN by high-resolution XRD measurement. (**a**) (0002) ω scan, (**b**) (10−11) ω scan.

We performed PL measurement from 10 K to 250 K. The PL measurements are carried out through a 0.75 m monochromator with a high resolution about 0.01 nm in 400 nm (about 0.078 meV), and a low-temperature sample stage cooled by a Helium Closed Cycle Cryostat with a temperature accuracy within ±1 degree. The excitation source is a He-Cd laser with 325 nm, which can be focused to a small area of about 10 µm in diameter. Because the dislocation density of $10^5/cm^2$ is equivalent to an average distance of 30 micrometer between two adjacent dislocations, the focus spot area is dislocation free with high possibility. The PL spectrum of the GaN/GaN sample is shown in Figure 2. From this, the variation curve of the actual GaN band edge exciton energy as a function of temperature (E-T curve) can be obtained.

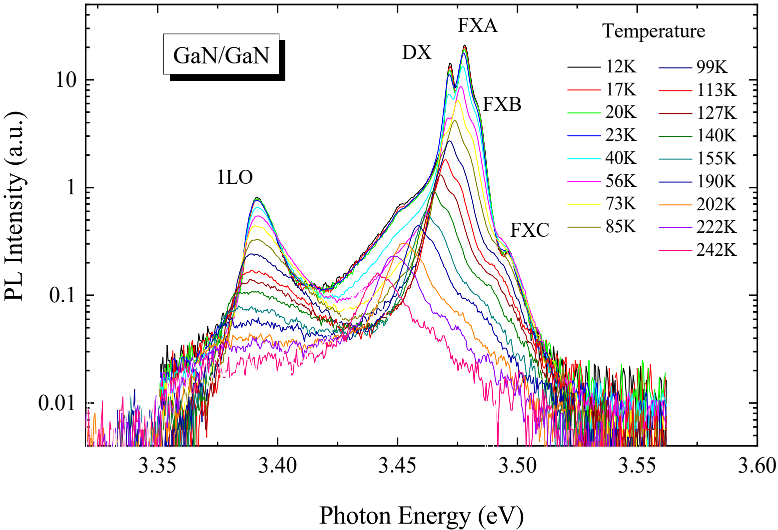

Figure 2. The temperate-dependent PL spectrum of the GaN/GaN sample.

3. Calculations and Models

3.1. Early Models

3.1.1. Varshni's Model

In studies of semiconductor exciton energy and temperature, we must mention the earliest fitting equation, known as Varshni's formula. This formula serves as an approximate model for the two behavioral models proposed by Varshni for the Eg-T curve at low and high temperatures [24,35]. Since its introduction, it has become the most widely used fitting formula for the relationship between energy bands and temperature in semiconductors. The equation is as below:

$$E_g(T) = E_0 - \frac{\alpha \times T^2}{\beta + T} \tag{1}$$

In Equation (1), the parameter E_0 represents the exciton energy at 0 K, and the parameter α is the energy band contraction coefficient at high temperature, or the slope of the fitted line at high temperature. The fitting result of the parameter β is widely considered to be related to the Debye temperature of the material studied. In the study of GaAs, the fitted parameter β represents its Debye temperature.

We begin by using Varshni's model to conduct fitting studies on our data. The fitting results are shown in the solid black line in Figure 3a. We can see that the fitting results exhibit significant deviations across various temperature ranges. Specifically, the fitted values are higher than the experimental data in the temperature range below 40 K and lower in the temperature range from 40 K to 120 K. The energy deviations are shown in Figure 3b. This type of deviation is not a random error; therefore, it should not be attributed to measurement or fitting errors, but rather, it reflects a systematic error related to the underlying mechanism. Another indication is that as we see the fitting parameters in Table 1, the fitting result of α is 19, and the apparently abnormal number of β is as high as 2509. However, by comparing past fitting results of Varshni's formula to GaN, we find that there is a wide range of distribution of the fitting parameter α and β, and even negative numbers that are difficult to explain in terms of physical principle. In the study of traditional narrow bandgap semiconductor materials, Varshni's formula has demonstrated exceptional performance, but it is notably inadequate for wide bandgap semiconductor materials like GaN. Therefore, Varshni's mode is not a suitable model to study the energy of GaN excitons. The reason for this is mainly that its mathematical expression is overly simplistic and does not take into account the characteristic parameters of GaN material. It

only contains three parameters that have no actual physical significance, which makes it insufficient to adequately characterize the behavior of GaN excitons at both low and high temperatures.

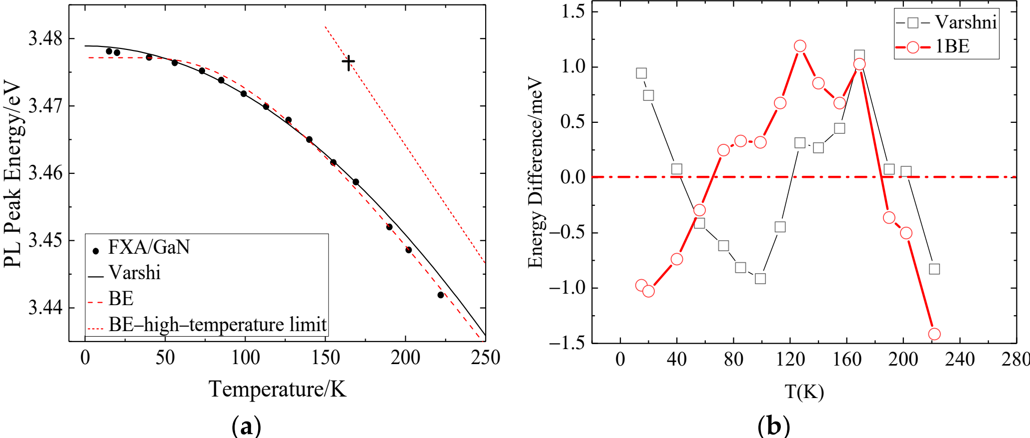

Figure 3. (**a**) Comparison of the fitting results of the A free exciton energy of GaN materials using Equations (1) and (2) in the temperature range of 0−230 K. The straight line in the figure is the high temperature limit of the type 2 line. The straight line passes through Eg (0), and the cross mark represents the feature point (T = θ/2). The black dots are the experimental data, and the black curved line is the fitting result of Equation (1). The red dashed line is the fitting result of Equation (2). (**b**) Errors of the fitting results of Equations (1) and (2) compared with experimental data at different temperatures. The square black box represents the error of Equation (1), and the red circles represent the error of Equation (2). The ordinate represents the difference between the experimental data and the fitted data.

Table 1. Parameters from different models.

Equation	E_0 (eV)	α (eV/K)	β/θ (K)	θ_2 (K)	P/r/ω	Kθ (meV)	R^2
(1)	3.4789	19	2509			216.2	0.996
(2)	3.47716	3.52	325.94			27.99	0.993
(4)	3.47779	5.7	138	645	0.211		0.9995
(6)	3.478	5.7	478.96		0.46559	41.238	0.9997
(7)	3.47809	18	1581		2.24	136.124	0.9996
(8)	3.47825	5.8	711		0.465		0.9996

3.1.2. Bose–Einstein Model (1BE Model)

Starting with the Bose–Einstein model, Vina proposed another alternative model. The fit is as follows [35,36]:

$$E_g(T) = E_B - a_B\left(1 + \frac{2}{\exp\left(\frac{\theta}{T}\right) - 1}\right) \equiv E_g(0) - \frac{\alpha\theta}{2}\left(\coth\left(\frac{\theta}{2T}\right) - 1\right) \quad (2)$$

Another version of this formula can be obtained from Equation $2 \times (\exp(x) - 1)^{-1} = \left(\coth\left(\frac{x}{2}\right) - 1\right)$. The bandgap limit at $T = 0$ is given by $E_g(0) = E_B - a_B$, where $\alpha = 2a_B/\theta$ is the contraction coefficient of the limit bandgap; and θ represents the effective phonon temperature, which is related to the average frequency of the acoustic branch and the optical branch by $\kappa T = h\omega$. Compared to the Varshni model, it at least introduces the physically meaningful concept of phonon temperature, albeit only as an average effect.

However, the results in Figure 3a (red dashed line) indicate a noticeable deviation across all temperature ranges, which is also evident in Figure 3b. The fitting result of the BE model in the temperature section before 40 K tends to be constant because when

$T \overset{\Delta}{\rightarrow} 0$, there is a mathematical expression $\left(exp\left(\frac{\theta}{T}\right) - 1\right)^{-1} \overset{\Delta}{\rightarrow} 0$. So, this model is clearly unreasonable at low temperatures.

The model performs well in the temperature range above 110 K because its physical parameters hold certain physical significance. As a result, the fitting parameters are more reasonable than those in the Varshni formula. However, even so, the formula proposed by Vina is still inadequate for describing the relationship between the exciton energy of GaN and temperature. These results indicate that it is necessary to start with the correct physical mechanisms, select parameters with physical significance, and establish a mathematical model to study the relationship between exciton energy and temperature in GaN.

3.2. Novel Model

Both the Varshni model and the Bose–Einstein model are empirical models that lack a consideration of physical mechanisms, which makes their models have poor applicability in wide bandgap materials. It has been known that the energy band shifts with temperature due to the following two main factors: thermal expansion of the lattice and the interaction between electrons and phonons. Generally, the contribution from thermal expansion is relatively minor, allowing us to overlook it, while the interaction between electrons and phonons is the primary influencing factor [8,37].

From this point of view, a group has proposed the following primitive integration [38]:

$$E_g = E_B - \int d\varepsilon f(\varepsilon)\left(\frac{1}{2} + \overline{n}(\varepsilon, T)\right) = E_g(0) - \frac{1}{2}\int d\varepsilon f(\varepsilon)\left(\coth\left(\frac{\varepsilon}{2KT}\right) - 1\right) \quad (3)$$

where ε is energy and $\overline{n}(\varepsilon, T)$ is the average number of phonons or the probability of occupying phonons in the energy ε. $f(\varepsilon) \propto \mathrm{D}(\varepsilon) \times \rho(\varepsilon)$,D(ε) is the coupling coefficient of electron phonon interaction which is often summed up as a constant, and ρ(ε) is the density of phonon states. For different semiconductor materials, it is important to properly mathematically represent the phonon density of states. Unfortunately, this remains unclear for GaN.

3.2.1. Singular Model (2BE Model)

A plausible approach for estimating the density of phonon states in GaN materials is to employ singular functions for generalization. When we use a singular function to express the phonon density of its acoustic phonons and optical phonons, that is, $f(\varepsilon) \propto \mathrm{C}\delta(\varepsilon - \varepsilon_0)$, the integral result is the Bose–Einstein model of (2). But the above fitting result of (2) is not good. Then, when we use two singular functions, $\delta(\varepsilon - \varepsilon_1)$ and $\delta(\varepsilon - \varepsilon_2)$, we represent the phonon density at the low energy end and the high energy end, respectively. That is $f(\varepsilon) \propto \mathrm{C}\delta(\varepsilon - \varepsilon_1) + \mathrm{D}\delta(\varepsilon - \varepsilon_2)$, substituting the original approximate integral result as follows:

$$E(T) = E_0 - \alpha\left(\frac{\omega\theta_1}{exp\left(\frac{\theta_1}{T}\right) - 1} + (1 - \omega)\frac{\theta_2}{\exp\left(\frac{\theta_2}{T}\right) - 1}\right) \quad (4)$$

We call this the 2BE model. In Equation (4), E_0 represents the bandgap energy at 0 K; α represents the high energy band shrinkage factor; θ_1 and θ_2 represent the effective phonon temperature of the acoustic branch and the optical branch, respectively; and ω, $1 - \omega$ represents the acoustic branch and the optical Branches contribute to the band offset.

It can be seen from Figure 4a that the fitting curve of the 2BE model is closer to the experimental data than to the 1BE model. The error analysis and comparison of the illustration also shows that the error of the 2BE model is smaller than that of the 1BE model in almost the entire temperature range, and the range of energy error dispersion is smaller. There is no obvious system deviation. The fitting parameters θ_1 and θ_2 are 138 K and 645

K, respectively. It can be concluded that the effective energy of the acoustic phonon is 11.9 meV and the energy of the optical phonon is 55.6 meV. These are closer to the actual energy of the GaN phonons, although there are still some differences. The ω is 0.211, which means that in the variation in exciton energy of GaN with temperature, optical phonons play a major role. Better fitting patterns, smaller fitting errors, and fitting parameters with reasonable physical meanings indicate that the 2BE model demonstrates good performance in GaN E-T curve analysis.

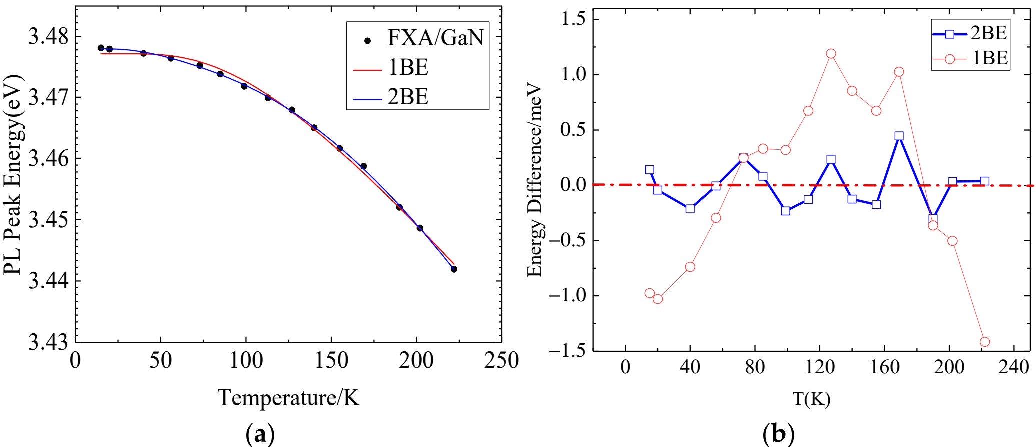

Figure 4. (**a**) Comparison of the fitting results of 1BE and 2BE to GaN materials. The red curve in the figure is the fitting result of 1BE, and the blue curve is the fitting result of 2BE. Black dots are experimental data. (**b**) Error comparison between the fitted data and the experimental data for 1BE and 2BE. The ordinate represents the difference between the experimental data and the fitted data. The red circles indicate the error of the 1BE model, and the blue squares indicate the error of 2BE.

3.2.2. Linear Model

In addition to singular functions, we can use a linear function to mathematically express the density of phonon states, such as $(\varepsilon) \propto C\varepsilon$, substituting the original integral formula, and the integral approximation result as follows:

$$E_g(T) = E_g(0) - \frac{\alpha\theta}{2} \times \left[\sqrt[4]{1 + \frac{\pi^2}{6} \times \left(\frac{2T}{\theta}\right)^2 + \left(\frac{2T}{\theta}\right)^4} - 1 \right] \tag{5}$$

In Equation (5), $E_g(0)$ represents the energy of excitons at 0 K. α represents the contraction coefficient of the energy band at high temperature, and θ represents the effective phonon temperature. The result of fitting using Equation (5) is shown in Figure 5. The fitted result is not very good. From the perspective of the entire fitting temperature range, there is a relatively large error, and the magnitude of the parameters we fit out also fail to represent the physical meaning. Therefore, simply using a linear function to summarize the density of the phonon states of GaN does not achieve the desired fitting effect.

3.2.3. Power-Law Model

Typically, the density of state distribution is unlikely to be linear, while a power distribution is more representative of actual conditions. In fact, the power functions are often used to describe the phonon density of semiconductor materials. We describe the density of the phonon states of GaN materials by constructing different power functions, then perform a mathematical derivation and use the resulting integral formula to fit the experimental data.

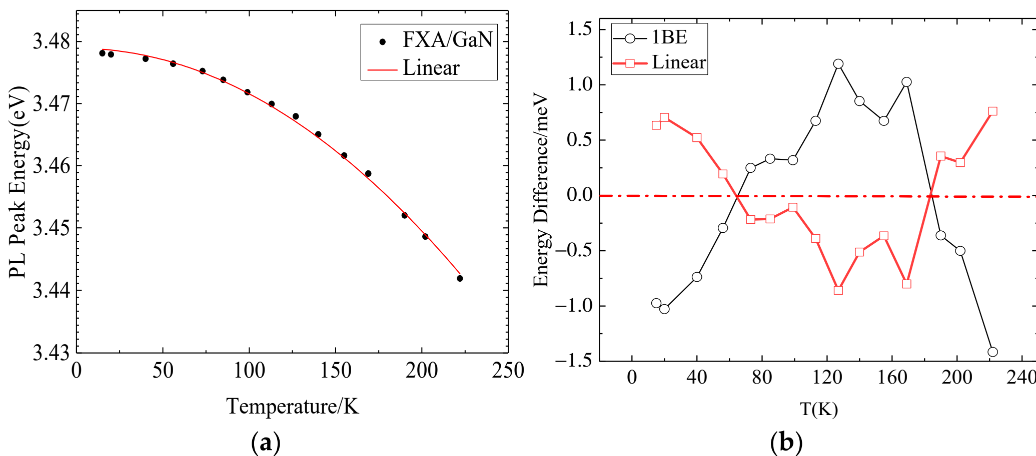

Figure 5. (**a**) Fit of the experimental data using a linear model. Black dots represent the actual measured experimental data, and red solid lines represent the fitted curves. (**b**) Error comparison between the fitted data and the experimental data for 1BE and linear model. The ordinate represents the difference between the experimental data and the fitted data. The red squares indicate the error of the linear model, and the black circles indicate the error of 1BE.

(a) Power-law-delta model

The density of the phonon states of GaN is described in the form of $f(\varepsilon) \propto \frac{C\varepsilon}{(\varepsilon_0-\varepsilon)^{\delta}}$, where $0 < \delta < 1$, ε_0 represents the cutoff energy, and the integration result in the energy range greater than ε_0 is zero. We derive the integral approximation result for this equation as follows:

$$E_g(T) = E_g(0) - \frac{\alpha\theta}{2} \times \left[\sqrt[4]{1 + 2r \times \left(\frac{2T}{\theta}\right)^2 + \left(\frac{2T}{\theta}\right)^4} - 1 \right] \quad (6)$$

In Equation (6), $r = \frac{(1-\delta)}{(2-\delta)}\frac{\pi^2}{6}$. $E_g(0)$, α, θ in the formula has the same physical meaning as before. Using Equation (6) to fit the experimental data, the fitting pattern of Figure 6 is obtained. It can be seen from the figure that the fitting data are closer to the experimental data. R^2 values as high as 0.9997 also mean that the fit is very successful. The effective phonon temperature of 478.96 K and the phonon energy of 41.238 meV are also in the reasonable energy range of the GaN phonon. This shows that the model can successfully perform mathematical analysis for the exciton energy of GaN and can obtain fitting parameters with reasonable physical meaning.

(b) Power-law-v model

In addition to the power function constructed above, we can also try to describe the phonon density of GaN in the form of $f(\varepsilon) \propto C\varepsilon^{\nu}$. When certain conditions are satisfied, the integral approximation result can be expressed as follows:

$$E_g(T) = E_g(0) - \frac{\alpha\theta}{2} \times \left[\sqrt[p]{1 + \left(\frac{2T}{\theta}\right)^p} - 1 \right] \quad (7)$$

Among them, $p = \nu + 1$, and the condition to be satisfied is that p is less than 2.5. $E_g(0)$, α, θ have the same physical meaning.

The fitting result is shown in Figure 7. Obviously, the fitting effect is relatively good. From the fitting parameters, although the R^2 value of 0.996 is appropriate and the p value satisfies the approximate condition, the fitted α, θ values are all too large, especially the effective phonon temperature θ, which is as high as 1581 K and indicates a phonon energy

of 136 meV. Thus, the fitted result does not represent the actual physical state of GaN, and the $C\varepsilon^{\nu}$ description of the phonon density of states does not provide a good picture of the actual phonon density of GaN.

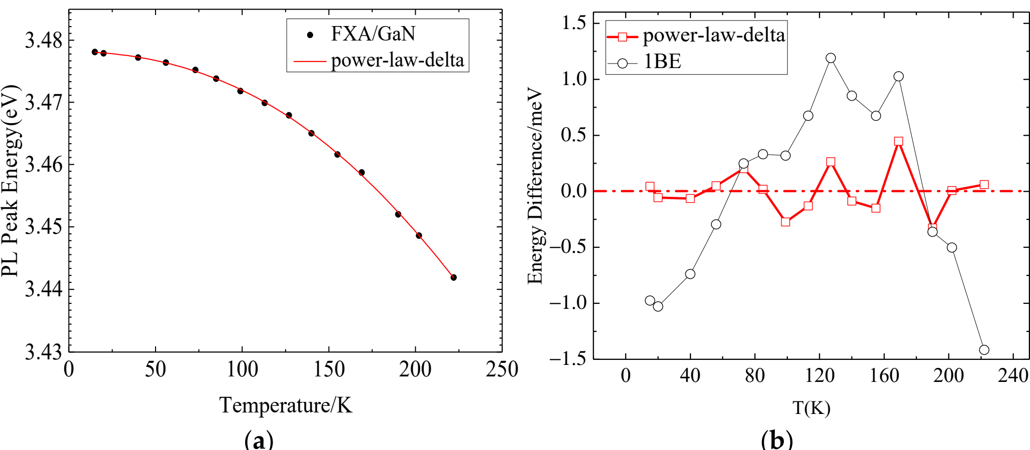

Figure 6. (**a**) Results obtained by fitting the experimental data to the power-law-delta model. The black dots represent the experimental data actually measured, and the solid red lines represent the fitted curves. (**b**) Error comparison between the fitted data and the experimental data for 1BE and power-law-delta model. The ordinate represents the difference between the experimental data and the fitted data. The red squares indicate the error of the power-law-delta model, and the black circles indicate the error of 1BE.

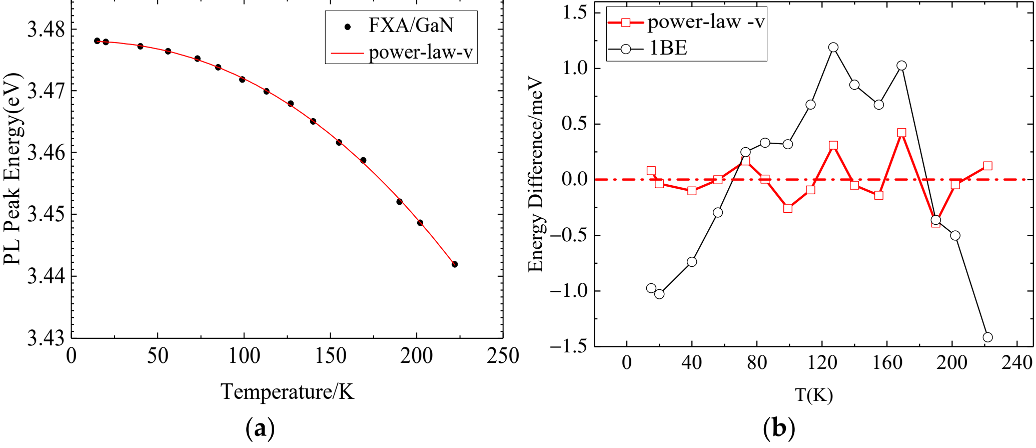

Figure 7. (**a**) Power-law-v model fitted to experimental data. The black dots represent the experimental data actually measured, and the solid red line represents the fitted curve. (**b**) Error comparison between the fitted data and the experimental data for 1BE and power-law-v model. The ordinate represents the difference between the experimental data and the fitted data. The red squares indicate the error of the power-law-v model, and the black circles indicate the error of 1BE.

3.2.4. Singular-Linear Model

Although neither the singular function nor the linear function is sufficient to describe the phonon density of GaN individually, we can still improve them. We can fully utilize their respective rationality and combine them to describe the phonon density of GaN. Take $f(\varepsilon) \propto \frac{\alpha}{k_b}\left(w\frac{\varepsilon}{\varepsilon_0} + (1-w)\varepsilon_0\delta(\varepsilon-\varepsilon_0)\right)$ as an example, where the first term represents the low-end contribution of the acoustic phonon and the second term represents the

contributions of the acoustic phonon of the high-energy end and the optical phonon. The approximate integration results are expressed as follows:

$$Eg(T) = Eg(0) - \frac{\alpha\theta_0}{2} \times \left[\frac{\omega}{2} \times \left(\sqrt[4]{1 + \frac{\pi^2}{6} \times \left(\frac{4T}{\theta_0}\right)^2 + \left(\frac{4T}{\theta_0}\right)^4} - 1\right) + (1-\omega)\times \left(\coth\left(\frac{\theta_0}{2T}\right) - 1\right)\right] \quad (8)$$

where $E_g(0)$, α has the same physical meaning. The effective phonon temperature is represented by $\left(1 - \frac{1}{2}\omega\right)\theta$, where ω represents the weight of the contribution.

It can be seen from Figure 8 that its fitting effect is good. ω = 0.465, indicating that the phonon contribution at the low energy end is lower compared with the 0.211 contribution weight of the 2BE model, which is slightly larger. Nevertheless, it still shows that the high energy terminator plays a major role. From θ = 711 K, the effective phonon temperature is 546 K, and the effective phonon energy is 47 meV. This is within the range of high-energy and low-energy phonons. This shows that the singular-linear model can be applied in the exciton study of GaN materials.

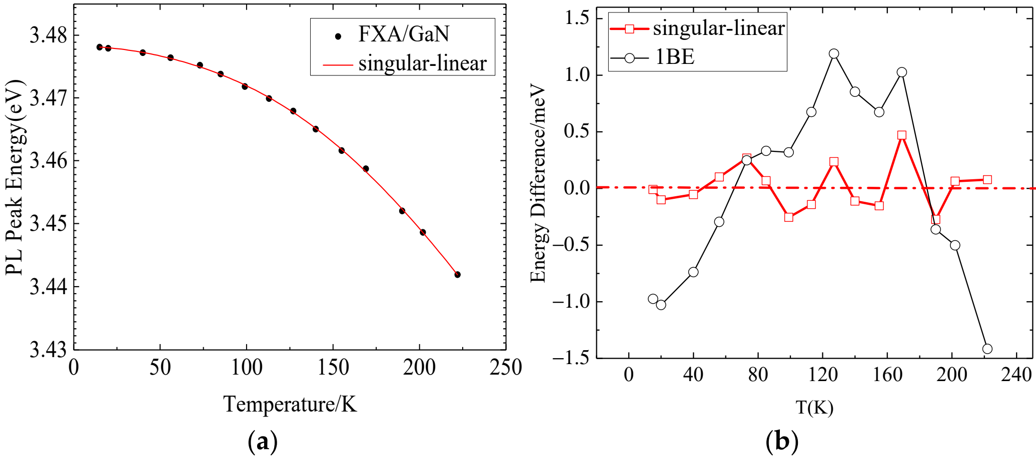

Figure 8. (**a**) Resulting plot of a singular-linear model fitted to the experimental data. Black dots represent the experimental data actually measured. The solid red line represents the fitted curve. (**b**) Error comparison between the fitted data and the experimental data for 1BE and singular-linear. The ordinate represents the difference between the experimental data and the fitted data. The red squares indicate the error of the singular-linear model, and the black circles indicate the error of 1BE.

4. Discussion

The precise experimental measurements and comparisons with various model fittings allowed us to find a mathematical model that properly examined the relationship between GaN exciton energy and temperature. Basically, there are two types of behavioral patterns of exciton energy with temperature. At low temperatures, $E_g(T) \to E_g(0) - \frac{1}{2} \times E_g''(0)T^2$ exhibiting quadratic behavior, and $E_g(T) \to H_g - \alpha T$ at high temperatures, exhibiting linear behavior, where $H_g, \alpha, E_g(0), E_g''(0)$ characterize two behavior patterns as four independent variables. Of course, more parameters with physical and mathematical significance are better for establishing models. But more importantly, building a model needs to be based on effective physical mechanisms, and the fitting parameters need to have physical meaning and be consistent with known ranges.

The physical mechanism of bandgap narrowing is primarily driven by electron–phonon interactions. By utilizing the electron–phonon spectral function, which describes the relationship between electrons and phonons, we can flexibly conduct theoretical analyses of the temperature dependence of the bandgap $Eg(T)$ in GaN structures. However, the

key lies in finding an appropriate form of the electron–phonon spectral function that can effectively describe the phonon density of states in GaN materials. This choice will directly influence the expression and understanding of the physical mechanism of the bandgap narrowing in GaN materials.

The Varshni model's physical assumptions lack a solid physical foundation. The results indicate that at low temperatures, the model underestimates the temperature dependence of the GaN bandgap, leading to an overall overestimation of the fitted data. At high temperatures, it overestimates the temperature dependence of the bandgap, increasingly deviating from physical reality. This is reflected in the model's predictions for the GaN bandgap energy, which diverge further from experimental measurements as the temperature rises. Therefore, this model is not suitable for studying the temperature dependence of the GaN bandgap.

The Bose–Einstein model (1BE) considers part of the physical reality. However, its overly simplistic mathematical formulation leads to an exaggerated estimation of the temperature dependence of the GaN bandgap at low temperatures. As a result, the fitting results of this model exhibit a systematic underestimation of experimental data in the low-temperature region below 40 K. Moreover, throughout the entire temperature range we investigated, the model shows recurring systematic deviations. Therefore, this model is also not suitable for studying the temperature dependence of the GaN bandgap.

The 2BE model takes into account the division of the GaN phonon spectrum into high-energy and low-energy segments, using two singular functions to represent the density of states at the low and high energy ends of the phonon spectrum. This approach aligns more closely with the actual phonon density of states in GaN. The fitting curve of the 2BE model is also better matched to the experimental data. Throughout the entire temperature range of the study, the error of the 2BE model is smaller than that of the 1BE model, and the errors are uniformly distributed across both positive and negative ranges, with no significant systematic bias.

The linear electron–phonon spectral function of the linear model does not accurately describe the phonon density of states in GaN. This model not only deviates from the experimental observations in its mathematical estimation of the temperature dependence of the GaN bandgap but also yields fitting parameters that exhibit unrealistic physical inferences.

Although the power-law model of the electron–phonon spectral function can effectively predict the experimental data on the temperature dependence of the GaN bandgap in its physical fitting images, its limitation lies in the assumption that the effective phonon energy primarily influencing the temperature dependence of GaN is 136.124 meV from power-law-v model. This effective phonon energy significantly exceeds the edge energy of the GaN phonon spectrum, which is about 95 meV, and clearly does not align with the physical realities of GaN. The power-law-delta model avoids this problem and implies the significance of the delta function. Therefore, while the power-law model performs well in terms of fitting, it has considerable deviations in terms of physical interpretation and the practical significance of its effective parameters, suggesting that we need to be more cautious when analyzing the phonon characteristics of GaN by the models.

The combined model of linear functions and singular functions utilizes linear function forms to represent the density of states of transverse acoustic phonons and long-wavelength longitudinal acoustic phonons, while singular function forms are used to characterize the optical phonons and short-wavelength longitudinal acoustic phonons. The conclusions drawn from fitting the temperature dependence of the GaN bandgap using this approach are more reliable.

In addition, the thermal expansion of the lattice is a problem that we need to consider. The thermal expansion of the lattice is mainly caused by the longitudinal acoustic phonons.

If one fitting model does not consider the role of longitudinal acoustic phonons, it is not appropriate. However, our combined model of linear functions and singular functions has included the influence from all phonons; the fitting process also includes the influence of lattice thermal expansion. Therefore, we do not need to additionally consider the influence of lattice thermal expansion.

Figure 9 shows the comparison of the error between the fitting results of Equations (1), (2), (4)–(8), and the experimental data at different temperatures. The error analysis shows that the errors of 2BE, power-law-delta, power-law-v, linear model, and singular-linear models are smaller than that of the 1BE and Varshni models in almost the entire temperature range. Compared to all forms of density of state representation, we believe that the 2BE and singular-linear models can more accurately indicate the competitive contributions of various phonons to the temperature dependence of the GaN bandgap.

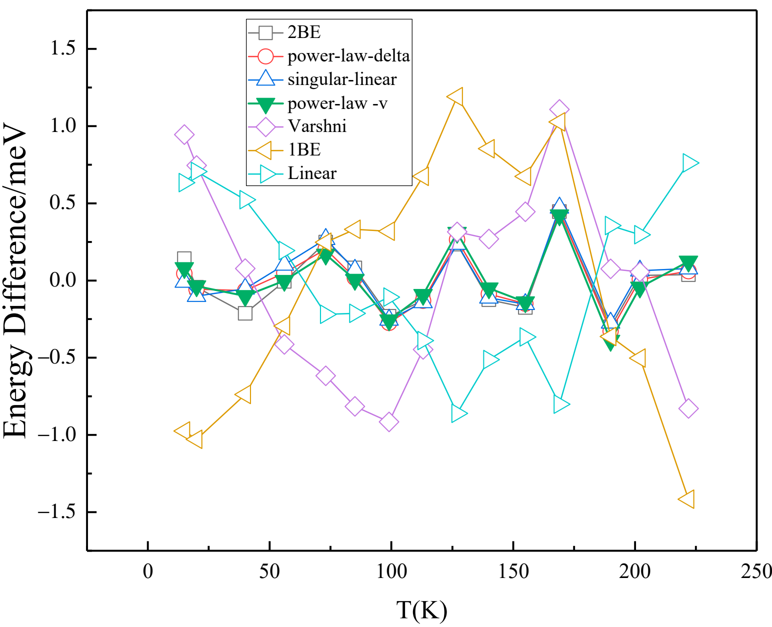

Figure 9. Comparison of the error between the fitting results of Equations (1), (2), (4)–(8), and the experimental data at different temperatures. The ordinate represents the difference between the experimental data and the fitted data.

5. Conclusions

Based on the measurements of high-quality GaN materials, we utilized 2BE, power-law-delta, power-law-v, and singular-linear models for fitting, and concluded that the electron–phonon interaction plays a decisive role in the temperature dependence of the exciton energy at the band edge of GaN. A comparison of the fundamental physical mechanisms and the fitting results reveals that the model which fully takes into account the various phonon interactions is a better choice. Many studies have shown that phonon characteristics have a significant impact on the thermoelectric properties of semiconductor devices under various operating conditions. The theoretical results based on electron–phonon interactions are of profound significance for the design of semiconductor devices. This research indicates that we can utilize the combined singular-linear model to analyze the relevant phonon characteristics, which will enable us to infer unknown phonon spectra and the distribution of phonon modes in other materials or physical structures. This will help us gain a more comprehensive understanding of the close relationship between these phonon characteristics and optoelectronic properties, providing theoretical support for the optimization and performance enhancement of new materials.

Author Contributions: Conceptualization, P.C.; formal analysis, X.L.; methodology, X.L., Z.X., D.C., X.X. and H.Z.; software, X.L.; investigation, P.C.; resources, P.C.; data curation, P.C.; writing—original draft preparation, P.C.; writing—review and editing, P.C.; supervision, Y.S., R.Z. and Y.Z.; project administration, P.C.; funding acquisition, P.C. All authors have read and agreed to the published version of the manuscript.

Funding: This research was funded by the National Nature Science Foundation of China, grant number 12074182; and the Collaborative Innovation Center of Solid-State Lighting and Energy-saving Electronics and Open Fund of the State Key Laboratory on Integrated Optoelectronics, grant number IOSKL2017KF03.

Data Availability Statement: All data, theory details, and simulation details that support the findings of this study are available from the corresponding authors upon reasonable request.

Acknowledgments: The authors acknowledge Nanjing University and the Jiangsu Provincial Key Laboratory of Advanced Photonic and Electronic Materials for their support in advanced micro technology and clean room facilities.

Conflicts of Interest: The authors declare no conflicts of interest.

References

1. Boutramine, A. Temperature-and Composition-Dependent Band Gap Energy and Electron–Phonon Coupling in InAs1−xSbx Semiconductors Alloys for Infrared Photodetection. *J. Electron. Mater.* **2023**, *52*, 6031–6041. [CrossRef]
2. Isik, M.; Gasanly, N.M.; Darvishov, N.H.; Bagiev, V.E. Effect of temperature on band gap of $PbWo_4$ single crystals grown by Czochralski method. *Phys. Scr.* **2022**, *97*, 45803. [CrossRef]
3. Kumar, A.; Kumar, S.; Miyai, Y.; Shimada, K. Temperature-dependent band modification and energy dependence of the electron-phonon interaction in the topological surface state on Bi_2Te_3. *Phys. Rev. B* **2022**, *106*, 121104. [CrossRef]
4. Surucu, O.; Isik, M.; Terlemezoglu, M.; Bektas, T.; Gasanly, N.M.; Parlak, M. Temperature effects on optical characteristics of thermally evaporated $CuSbSe_2$ thin films for solar cell applications. *Opt. Mater.* **2022**, *133*, 113047. [CrossRef]
5. Wu, R.; Ma, M.; Zhang, S.; Zhao, P.; Li, K.; Zhao, Q.; Chang, A.; Zhang, B. Enhanced linearity of $CaCu_3Ti_4O_{12}$ by changing energy band structure induced by Fe^{3+} doping for high temperature thermistor application. *Appl. Phys. Lett.* **2022**, *121*, 96124. [CrossRef]
6. Tamariz, S.; Callsen, G.; Stachurski, J.; Shojiki, K.; Butté, R.; Grandjean, N. Toward Bright and Pure Single Photon Emitters at 300 K Based on GaN Quantum Dots on Silicon. *ACS Photonics* **2020**, *7*, 1515–1522. [CrossRef]
7. Deng, J.; Yu, J.; Hao, Z.; Kang, J.; Lu, B.; Wang, L.; Sun, C.; Han, Y.; Xiong, B.; Wang, J.; et al. Disk-Shaped GaN Quantum Dots Embedded in AlN Nanowires for Room-Temperature Single-Photon Emitters Applicable to Quantum Information Technology. *ACS Appl. Nano Mater.* **2022**, *5*, 4000–4008. [CrossRef]
8. Allen, P.B.; Cardona, M. Temperature dependence of the direct gap of Si and Ge. *Phys. Rev. B* **1983**, *27*, 4760–4769. [CrossRef]
9. Hartel, A.M.; Gutsch, S.; Hiller, D.; Zacharias, M. Fundamental temperature-dependent properties of the Si nanocrystal band gap. *Phys. Rev. B* **2012**, *85*, 165306. [CrossRef]
10. Klenner, M.; Falter, C.; Ludwig, W. Temperature dependence of band gaps in Si and Ge in the quasiion model. *Ann. Phys.* **2006**, *504*, 34–38. [CrossRef]
11. Lautenschlager, P.; Allen, P.B.; Cardona, M. Temperature dependence of band gaps in Si and Ge. *Phys. Rev. B* **1985**, *31*, 2163–2171. [CrossRef] [PubMed]
12. Vainorius, N.; Kubitza, S.; Lehmann, S.; Samuelson, L.; Dick, K.A.; Pistol, M.-E. Temperature dependent electronic band structure of wurtzite GaAs nanowires. *Nanoscale* **2018**, *10*, 1481–1486. [CrossRef] [PubMed]
13. Pavesi, L.; Piazza, F.; Rudra, A.; Carlin, J.F.; Ilegems, M. Temperature dependence of the InP band gap from a photoluminescence study. *Phys. Rev. B* **1991**, *44*, 9052–9055. [CrossRef]
14. Rong, X.; Lu, Y.; Yin, J.; Jiang, H.; Han, S.; Zeng, Y.; Xu, W.; Fang, M.; Cao, P.; Zhu, D.; et al. Electroluminescence enhancement of ZnO nanorod array/GaN heterojunction with MgZnO barrier layer. *J. Lumin.* **2022**, *248*, 118946. [CrossRef]
15. Xu, R.; Chen, P.; Zhou, J.; Li, Y.; Li, Y.; Zhu, T.; Cheng, K.; Chen, D.; Xie, Z.; Ye, J.; et al. High Power Figure-of-Merit, 10.6-kV AlGaN/GaN Lateral Schottky Barrier Diode with Single Channel and Sub-100-µm Anode-to-Cathode Spacing. *Small* **2022**, *18*, e2107301. [CrossRef]
16. Xu, R.; Chen, P.; Liu, M.H.; Zhou, J.; Yang, Y.F.; Li, Y.M.; Ge, C.; Peng, H.C.; Liu, B.; Chen, D.J.; et al. 1.4-kV Quasi-Vertical GaN Schottky Barrier Diode With Reverse Junction Termination. *IEEE J. Electron Devices Soc.* **2020**, *8*, 316–320. [CrossRef]
17. Xu, R.; Chen, P.; Liu, M.H.; Zhou, J.; Li, Y.M.; Liu, B.; Chen, D.J.; Xie, Z.L.; Zhang, R.; Zheng, Y.D. 2.7-kV AlGaN/GaN Schottky barrier diode on silicon substrate with recessed-anode structure. *Solid-State Electron.* **2021**, *175*, 107953. [CrossRef]

18. Patra, S.K.; Schulz, S. Exploring the Potential of c-Plane Indium Gallium Nitride Quantum Dots for Twin-Photon Emission. *Nano Lett.* **2020**, *20*, 234–241. [CrossRef]
19. Delphan, A.; Makhonin, M.N.; Isoniemi, T.; Walker, P.M.; Skolnick, M.S.; Krizhanovskii, D.N.; Skryabin, D.V.; Carlin, J.-F.; Grandjean, N.; Butté, R. Polariton lasing in AlGaN microring with GaN/AlGaN quantum wells. *APL Photonics* **2023**, *8*, 021302. [CrossRef]
20. Yang, J.; Tao, R.; Huang, Z.; Li, D.; Rong, X.; Chu, Z.; Liu, Q.; Huo, X.; Li, T.; Sheng, B.; et al. A near-resonant excitation strategy to achieve ultra-low threshold GaN polariton lasing. *Opt. Lett.* **2024**, *49*, 4058–4061. [CrossRef]
21. Xu, R.; Chen, P.; Liu, M.H.; Zhou, J.; Li, Y.M.; Cheng, K.; Liu, B.; Chen, D.J.; Xie, Z.L.; Zhang, R.; et al. 3.4-kV AlGaN/GaN Schottky Barrier Diode on Silicon Substrate With Engineered Anode Structure. *IEEE Electron Device Lett.* **2021**, *42*, 208–211. [CrossRef]
22. Xu, R.; Chen, P.; Liu, X.; Zhao, J.; Zhu, T.; Chen, D.; Xie, Z.; Ye, J.; Xiu, X.; Wan, F.; et al. A lateral AlGaN/GaN Schottky barrier diode with 0.36-V turn-on voltage and 10-kV breakdown voltage by using double-barrier anode structure. *Chip* **2024**, *3*, 100079. [CrossRef]
23. Vasileff, H.D. Electron Self-Energy and Temperature-Dependent Effective Masses in Semiconductors:n-Type Ge and Si. *Phys. Rev.* **1957**, *105*, 441–446. [CrossRef]
24. Pssler, R. Basic Model Relations for Temperature Dependencies of Fundamental Energy Gaps in Semiconductors. *Phys. Status Solidi B* **1997**, *200*, 155–172. [CrossRef]
25. Uesugi, K.; Suemune, I.; Hasegawa, T.; Akutagawa, T.; Nakamura, T. Temperature dependence of band gap energies of GaAsN alloys. *Appl. Phys. Lett.* **2000**, *76*, 1285–1287. [CrossRef]
26. Pässler, R. Temperature dependence of fundamental band gaps in group IV, III–V, and II–VI materials via a two-oscillator model. *J. Appl. Phys.* **2001**, *89*, 6235–6240. [CrossRef]
27. Zardas, G.E.; Yannakopoulos, P.H.; Ziska, M.; Symeonides, C.; Vesely, M.; Euthymiou, P.C. Temperature dependence of Si–GaAs energy gap using photoconductivity spectra. *Microelectron. J.* **2006**, *37*, 91–93. [CrossRef]
28. Pässler, R. Temperature dependence of exciton peak energies in multiple quantum wells. *J. Appl. Phys.* **1998**, *83*, 3356–3359. [CrossRef]
29. Liu, R.; Bayram, C. Cathodoluminescence study of luminescence centers in hexagonal and cubic phase GaN hetero-integrated on Si(100). *J. Appl. Phys.* **2016**, *120*, 025106. [CrossRef]
30. Na, J.H.; Taylor, R.A.; Rice, J.H.; Robinson, J.W.; Lee, K.H.; Park, Y.S.; Park, C.M.; Kang, T.W. Two-dimensional exciton behavior in GaN nanocolumns grown by molecular-beam epitaxy. *Appl. Phys. Lett.* **2005**, *86*, 123102. [CrossRef]
31. Viswanath, A.K.; Lee, J.I.; Yu, S.; Kim, D.; Choi, Y.; Hong, C.-h. Photoluminescence studies of excitonic transitions in GaN epitaxial layers. *J. Appl. Phys.* **1998**, *84*, 3848–3859. [CrossRef]
32. Zhang, W.; Growden, T.A.; Berger, P.R.; Storm, D.F.; Meyer, D.J.; Brown, E.R. Temperature Characterization of Unipolar-Doped Electroluminescence in Vertical GaN/AlN Heterostructures. *Energies* **2021**, *14*, 6654. [CrossRef]
33. Cretì, A.; Tobaldi, D.M.; Lomascolo, M.; Tarantini, I.; Esposito, M.; Passaseo, A.; Tasco, V. Exciton Effects in Low-Barrier GaN/AlGaN Quantum Wells. *J. Phys. Chem. C* **2022**, *126*, 14727–14734. [CrossRef]
34. Boughrara, N.; Benzarti, Z.; Khalfallah, A.; Evaristo, M.; Cavaleiro, A. Comparative study on the nanomechanical behavior and physical properties influenced by the epitaxial growth mechanisms of GaN thin films. *Appl. Surf. Sci.* **2022**, *579*, 152188. [CrossRef]
35. Viña, L.; Logothetidis, S.; Cardona, M. Temperature dependence of the dielectric function of germanium. *Phys. Rev. B* **1984**, *30*, 1979–1991. [CrossRef]
36. Pässler, R. Alternative analytical descriptions of the temperature dependence of the energy gap in cadmium sulfide. *Phys. Status Solidi B* **2006**, *193*, 135–144. [CrossRef]
37. Collins, A.T.; Lawson, S.C.; Davies, G.; Kanda, H. Indirect Energy Gap of ^{13}C Diamond. *Phys. Rev. Lett.* **1990**, *65*, 891. [CrossRef]
38. O'Donnell, K.P.; Chen, X. Temperature dependence of semiconductor band gaps. *Appl. Phys. Lett.* **1991**, *58*, 2924–2926. [CrossRef]

Disclaimer/Publisher's Note: The statements, opinions and data contained in all publications are solely those of the individual author(s) and contributor(s) and not of MDPI and/or the editor(s). MDPI and/or the editor(s) disclaim responsibility for any injury to people or property resulting from any ideas, methods, instructions or products referred to in the content.